symmetry

IMPACT FACTOR 2.7

CITESCORE 4.9

Review

Antihydrogen and Hydrogen: Search for the Difference

Ksenia Khabarova, Artem Golovizin and Nikolay Kolachevsky

MDPI

https://doi.org/10.3390/sym15081603

symmetry

MDPI

Review

Antihydrogen and Hydrogen: Search for the Difference

Ksenia Khabarova [1,2], Artem Golovizin [1] and Nikolay Kolachevsky [1,2,*]

[1] P.N. Lebedev Physical Institute, Moscow 119991, Russia; k.khabarova@yandex.ru (K.K.); artem.golovizin@gmail.com (A.G.)
[2] Russian Quantum Center, Skolkovo, Moscow 121205, Russia
* Correspondence: kolachevsky@lebedev.ru

Abstract: Our universe consists mainly of regular matter, while the amount of antimatter seems to be negligible. The origin of this difference, known as the baryon asymmetry, remains undiscovered. Since the discovery of antimatter, many experiments have been carried out to study antiparticles and to compare matter and antimatter twins. Two of the most sensitive methods in physics, radiofrequency and optical spectroscopy, can be efficiently used to search for the difference. The successful synthesis and trapping of cold antihydrogen atoms opened the possibility of significantly increasing the sensitivity of matter/antimatter tests. This brief review focuses on a hydrogen/antihydrogen comparison using other independent spectroscopic measurements of single particles in traps and other simple atomic systems like positronium. Although no significant difference is detected in today's level of accuracy, one can push forward the sensitivity by improving the accuracy of 1S–2S positronium spectroscopy, spectroscopy of hyperfine transition in antihydrogen, and gravitational measurements.

Keywords: baryon asymmetry; antimatter; antihydrogen; 1S–2S spectroscopy; hyperfine spectroscopy; gravitation

PACS: 37.10.De; 37.10.Gh; 32.30.Jc

check for updates

Citation: Khabarova, K.; Golovizin, A.; Kolachevsky, N. Antihydrogen and Hydrogen: Search for the Difference. *Symmetry* **2023**, *15*, 1603. https://doi.org/10.3390/sym15081603

Academic Editor: Stefano Profumo

Received: 21 July 2023
Revised: 7 August 2023
Accepted: 14 August 2023
Published: 18 August 2023

1. Introduction

At the beginning of the 20th century, precision spectroscopic measurements of hydrogen atoms laid the foundation for the Dirac Equation [1], which is one of the most fundamental equations in quantum mechanics. Later, the brilliant spectroscopic experiments of Lamb and Rutherford (1947) triggered the development of quantum electrodynamics theory (QED). More and more accurate measurements of transition wavelengths and frequencies in atomic hydrogen and other simple atomic systems stimulated further development of QED, which today holds the position of the most accurate known theory. The combination of precision experiments with QED calculations resulted in extremely accurate values of the Rydberg constant, the fine structure constant α, the electron-to-proton mass ratio m_e/m_p, strict limitations to the drift of α, and many other results. In turn, the development of experimental spectroscopic methods caused the breakthrough in optical frequency measurements followed by the Nobel Prize for T.W. Hänsch and J. Hall in 2005. Precision spectroscopy of hydrogen atoms also occupies an important practical niche—hydrogen masers operating at the ground-state hyperfine transition (1.4 GHz) are the key instruments of national metrology laboratories and serve as on-board clocks for GALILEO global navigation satellites.

The discovery of the antimatter also goes back to the Dirac equation. Unexpectedly, the unification of the mathematical principles of quantum mechanics with the principles of special relativity resulted in the prediction of the positron. Four years later the positron was experimentally discovered by Anderson [2]. It is reasonable to suggest, that antimatter is the mathematical and physical twin of our regular matter and should follow the same laws of nature. The transformation from the matter world to the world of antimatter

can be performed by charge conjugation (C), parity transformation (P), and time reversal (T). Accordingly, all physical processes must be invariant over the CPT-transformation. Correspondingly, the transition from the photon epoch of the universe to matter domination (10 thousand years after the Big Bang) should deliver equal amounts of matter and anti-matter (leptons, hadrons, nuclei, etc.). In the 1970s, it was already clear that the observable universe consists predominantly of matter which contradicted the idea of symmetry. The puzzle of such a giant asymmetry, which allows our matter world to exist, is known as the baryon asymmetry problem.

The early stratospheric experiments showed that the positron fraction in cosmic rays does not exceed 10% [3]. The most advanced of today's experiments for direct observation of positrons (PAMELA [4], FERMI [5] and AMS [6] missions) confirmed that the positron fraction is at the level of 10% in the energy range 0.1–100 GeV. Positrons can be produced in the different nuclear processes in active astrophysical objects and reach the Earth afterward. The presence of antimatter in the universe can be also studied by indirect measurements, for example, by observation of the 511 keV line emitted in the annihilation process $e + \bar{e} \rightarrow 2\gamma$. The first observations of the 511 keV line were performed already in 1969 [7]. The full-scale mapping of the whole sky by the INTEGRAL mission excluded the existence of powerful annihilation sources which can be identified as massive fractions of antimatter [8].

At the same time, there is a search for baryon antimatter. The first stratospheric balloon experiments showed that the antiproton fraction in the cosmic rays is around 5×10^{-4} in 10 GeV range [9]. Later, the AMS02 mission improved these results and extended the energy range to 400 GeV [10]. Data analysis also showed a complete absence of antihelium nuclei in cosmic rays. For the whole observation period, there were only a few candidates with the charge of $Z = -2$ and a mass close to the mass of ^{3}He. One can draw the conclusion that the primordial sources of anti-matter in the visible universe do not exist and the whole anti-matter is of secondary origin. Accordingly, there is a common assumption, that the dominance of matter in the universe may be caused by an unknown asymmetry of physical laws for matter and antimatter [11]. Despite the great success of the standard model after the Higgs boson discovery, it does not explain the symmetry violation and the difference between matter and antimatter abundance. Probably, the violation of symmetry could happen at extremely high energies, which are close to the scale of great unification theories. Such energies are not accessible neither in accelerator laboratories, nor in astrophysical objects, which do not allow an experimental search for the CPT symmetry breaking.

Another approach to searching for the violations is high-precision experiments. Due to the extremely high accuracy and sensitivity of spectroscopic experiments, they are widely used for measuring CP-asymmetry [12], searching for the electron EDM [13], searching for variations of the fundamental constants [14], violations of the Lorentz symmetry [15], searching for dark matter [16], and many others (see the review [17]). For accurate spectroscopic measurements one needs relatively cold atoms of anti-hydrogen which were not available until early 2000.

In 2002, two CERN collaborations reported the successful synthesis of cold antihydrogen $\bar{\mathrm{H}}$, the atomic system consisting of a bound antiproton $\bar{\mathrm{p}}$, and a positron $\bar{\mathrm{e}}$. Finally, researchers had a unique opportunity to compare properties of matter and antimatter by the approved and extremely sensitive method—atomic spectroscopy. There is hope that increasing the measurement accuracy will reveal the difference and unveil the baryon asymmetry puzzle.

2. Positron and Anti-Proton

Before discussing anti-hydrogen production and spectroscopy measurements, one should briefly review fundamental tests performed on its constituents, namely a positron and an anti-proton. There are three main properties of a particle: the charge, the mass, and the magnetic moment, which were studied over the last years in different sensitive tests.

2.1. Charge

The equivalence of the positron's and the electron's charge directly follows from the annihilation reaction $e^+ + e^- \rightarrow 2\gamma$. Being of electromagnetic nature, the γ-quants are electrically neutral which must prove that e^- and e^+ charges (q_e and $q_{\bar{e}}$, respectively) are identical in modulo. To our knowledge, there were no dedicated experiments aimed at the comparison of q_e and $q_{\bar{e}}$. Some conclusions were made in the work [18], where the Rydbergs in positronium and hydrogen were compared. The authors derived that the charge ratio is restricted by $q_e/q_{\bar{e}} - 1 = 1(4) \times 10^{-8}$.

The equivalence of the electron and the proton charges was tested in a number of different experiments using neutral matter. In this case, the equivalence of charges becomes a more sophisticated question because the electron and the proton belong to different types of particles—leptons and baryons. The most stringent limit of $\epsilon_{e-p} = |q_e + q_p|/|q_e| < 10^{-21}$ was obtained experimentally by acoustic technique [19].

2.2. Mass

Precision radiofrequency measurements of particles loaded in the Penning trap allow for accurate measurements of the charge-to-mass ratio. The recent results on the proton/antiproton charge-to-mass ratios with the fractional uncertainty of 1.6×10^{-11} were reported in [20]. This result $-(q_p/m_p)/(q_{\bar{p}}/m_{\bar{p}}) - 1 = 3(16) \times 10^{-12}$ significantly improves the measurements performed by different groups (e.g., [21]) being the most stringent limitation for today.

The most accurate measurement of the antiproton-to-electron mass ratio is performed using two-photon spectroscopy of antiprotonic helium [22]. The experimental result gives $m_{\bar{p}}/m_e = 1836.1526736(23)$ which agrees within uncertainty with the proton-to-electron mass ratio $m_p/m_e = 1836.15267343(11)$ from CODATA [23]. Thus, the feasible difference between the antiproton and the proton mass is limited by $(m_{\bar{p}}/m_e)/(m_p/m_e) - 1 = m_{\bar{p}}/m_p - 1 = 0.1(1.2) \times 10^{-9}$.

Some conclusions about the positron and the electron masses can be made from experiments in the Penning trap where the charge-to-mass ratio of particles can be derived from the comparison of cyclotron frequencies. The result derived in [24] of $(q_e/m_e)/(q_{\bar{e}}/m_{\bar{e}}) - 1 < 1.3 \times 10^{-7}$ is based on the experimental results of P.B. Schwinberg et al. [25]. To our knowledge, it is the most stringent restriction even today. Other experiments aimed at direct comparison of the electron and positron masses are much less accurate (see. e.g., [26]).

2.3. Magnetic Moment

The magnetic moment of a particle is given by $\vec{\mu} = g(q/2m)\vec{S}$, where g is the particle's g-factor, q and m are the charge and the mass, correspondingly, and $\vec{S}$ is the spin angular momentum. For the Dirac particles $S = \hbar/2$.

For leptons (in our case e^- and $\bar{e}$), the g-factor can be calculated with very high accuracy using the framework of quantum electrodynamics. According to [27], the theoretical value equals $-g_e^{theo} = g_{\bar{e}}^{theo} = 2 \times 1.00115965218161(24)$ with the uncertainty of 2.4×10^{-13} in relative units. The experimental value of electron's g-factor $-g_e^{exp} = 2 \times 1.00115965218059(13)$ (1.3×10^{-13}) was obtained from spectroscopy of quantum jumps between the quantum energy levels of one electron suspended in a Penning trap [28]. The positron was characterized with a similar technique although with lower accuracy $g_{\bar{e}}^{exp} = 2 \times 1.0011596521879(43)$ (4.3×10^{-12}) [29]. The same experiments allowed putting the most stringent constriction for the electron-to-positron g-factor ratio of $|g_e^{exp}/g_{\bar{e}}^{exp}| - 1 = 0.5(2.1) \times 10^{-12}$. The reduction of relative uncertainty is related to common systematic effects for electrons and positrons alternatively loaded in the same trap [29]. The theoretical prediction is also consistent with both experimental results within corresponding uncertainties.

Due to the complex nature of the proton and anti-proton, their g-factors cannot be predicted with a reasonable accuracy. From the experimental side, spectroscopy in Penning traps gives impressive results, although it is much more difficult compared to electrons due to higher particle mass. Accurate experiments with protons made by G. Gabrielse's

group [30] paved the way for high-precision proton and antiproton spectroscopy. The accurate measurement of the proton magnetic moment $\mu_p/\mu_N \equiv g_p/2 = 2.792847350(9)$ (3.3×10^{-9} in relative units) was reported in 2014 [31] which was further improved in 2017 up to $\mu_p/\mu_N = 2.792847344\,62(82)$ (3×10^{-10}) [32]. The antiproton magnetic moment was also measured with high accuracy and is equal to $\mu_{\bar{p}}/\mu_N \equiv g_p/2 = -2.7928473441(42)$ (1.5×10^{-9}) [33]. There is no significant difference between g-factors of proton and antiproton down to the uncertainty of $(-g_p/g_{\bar{p}}) - 1 = 0.2(1.5) \times 10^{-9}$.

The results of electron/positron and proton/antiproton comparisons are summarized in Table 1.

Table 1. Experimental tests of electron-to-positron ($e - \bar{e}$) and proton-to-antiproton ($p - \bar{p}$) symmetry. Known most sensitive comparisons of mass (M), charge (q) and g-factors are given with 1σ uncertainty (68% confidence level).

|Parameter| −1	Restriction	References
q_p/q_e	$<10^{-21}$	[19]
$q_e/q_{\bar{e}}$	4×10^{-8}	[18]
$q_{\bar{p}}/q_{\bar{e}}$	7.1×10^{-10}	[34]
$(q_e/m_e)/(q_{\bar{e}}/m_{\bar{e}})$	1.3×10^{-7}	[25]
$(q_p/m_p)/(q_{\bar{p}}/m_{\bar{p}})$	1.6×10^{-11}	[20]
$m_e/m_{\bar{e}}$	1.4×10^{-7}	[18,25]
$m_p/m_{\bar{p}}$	1.2×10^{-9}	[22,23]
$g_e/g_{\bar{e}}$	2.1×10^{-12}	[29]
$g_p/g_{\bar{p}}$	1.5×10^{-9}	[33]

3. Laser Spectroscopy

3.1. Positronium

Spectroscopy remains one of the most powerful tools for precision measurements which can potentially reveal violations of fundamental theories [17] or discover new substances [35,36]. Pioneering experiments of measuring the 1S–2S transition in positronium (Ps) [37] showed already in 1984, that accurate laser measurements can be performed on anti-matter. Despite the short natural lifetime of ortho-Ps (142 ns), the 1S–2S frequency uncertainty reached 9×10^{-9} (in relative units). The result was improved later by a factor of 3 down to 2.6×10^{-9} [38]. Positronium, being a purely leptonic system, is one of the cornerstones for an accurate bound-state QED test. QED calculations of the 1S–2S frequency give the uncertainty of 5×10^{-10} [39], which competes with the uncertainty of the electron's magnetic moment calculations. Theory and experiment well match each other (within two standard deviations) which allows testing QED corrections up to the order of $m\alpha^6$. There are ongoing efforts to improve the experimental results of Ps spectroscopy [40,41], including 1S–2S frequency interval [42].

Alternatively, Ps spectroscopy can be used for searching the matter-antimatter asymmetry as shown in [18]. The energy scale for a two-particle system is given by the Rydberg constant

$$Ry = \frac{\mu e_1^2 e_2^2}{2\hbar^2}, \tag{1}$$

where $\mu = m_1 m_2/(m_1 + m_2)$ is the reduced mass of the two particles with masses m_1, m_2 and charges e_1 and e_2, respectively. It is convenient to introduce the reduced Rydberg $\bar{R}y$ as the ratio of (1) to the Rydberg for an atom with the infinite proton mass ($m_1 = m_e$, $m_2 = \infty$, $e_1 = e_2 = q_e$). For positronium we will get

$$\bar{R}y(\mathrm{Ps}) = \frac{(q_{\bar{e}}/q_e)^2}{m_e/m_{\bar{e}} + 1}. \tag{2}$$

Combining this equation together with the independent measurements of electron/positron cyclotron frequencies (Table 1, [25]), one can either set a restriction to $q_{\bar{e}}/q_e$ or to $m_{\bar{e}}/m_e$ similar to [18]. E.g., for $q_{\bar{e}}/q_e$ the restriction turns out to be equal to 3×10^{-7} with the dominating contribution of the cyclotron frequency comparison uncertainty (approximately $\frac{1}{5}$ th of it). This is very similar to the result published in [18], because the electron/positron cyclotron measurements were not improved since that. The limitation for the $m_{\bar{e}}/m_e$ can be obtained similarly and its uncertainty approaches $\frac{4}{5}$ th of the cyclotron frequency comparison uncertainty. If one assumes the strict electron/positron charge equivalence, the restriction to the mass ratio becomes as strong as for $\bar{R}y(\mathrm{Ps})$ or 3×10^{-9} in relative units.

One can see that 1S–2S spectroscopy in Ps basically tests the equivalence of Rydbergs (or the electron/positron rest energy mc^2 multiplied by the squared electromagnetic coupling constant α^2) in matter and anti-matter worlds.

Taking into account that the electron magnetic moment is given by the QED series

$$\mu_e/\mu_B = 1 + C_2(\alpha/\pi) + C_4(\alpha/\pi)^2 + \dots , \tag{3}$$

with the leading correction of $C_2(\alpha/\pi) = \alpha/2\pi$, one can use the results from Table 1 to compare the fine structure constants for matter (α) and anti-matter ($\bar{\alpha}$). The corresponding restriction is $|\bar{\alpha}/\alpha - 1| < 1.8 \times 10^{-9}$, which is $2\pi\alpha^{-1} \approx 860$ times larger than for the measured giromagnetic factor's ratio $g_{\bar{e}}/g_e$ [29]. Since $\alpha = e^2/\hbar c$ we obtain the corresponding restriction to the charge ratio of

$$|-q_{\bar{e}}/q_e - 1| < 9 \times 10^{-10} , \tag{4}$$

which is about 50 times more strict compared to the one from [18] (Table 1). Now, using (2) and the best result for Ps 1S–2S spectroscopy [38] one can also improve the restriction for $m_{\bar{e}}/m_e$ for the factor of 20 down to

$$|m_{\bar{e}}/m_e - 1| < 7 \times 10^{-9} . \tag{5}$$

There is ongoing work to improve the accuracy of the 1S–2S frequency measurement in positronium by one order of magnitude [42]. One of the main goals is to check the positron-to-electron mass equality on the new level of sensitivity. Still, due to the short lifetime of Ps, it is hard to expect many-digit improvement. A long-term dream of scientists has been the comparison of transition frequencies in hydrogen and anti-hydrogen. It became possible only after the successful synthesis and trapping of cold anti-hydrogen atoms.

3.2. Antihydrogen, 1S–2S

The first high-energy antihydrogen atoms were obtained in 1996 in relativistic collisions [43]. It took several decades to produce, trap, and cool antihydrogen atoms for direct comparison of matter and antimatter "twins". Effective cold anti-hydrogen production was realized at CERN in around 2010 by two groups, by mixing decelerated anti-protons and positrons in the Penning trap at 4 K [44–46]. It was demonstrated later that antihydrogen atoms can be magnetically trapped in the ground state for more than 1000 s using a magnetic bottle combined with an ion Penning trap.

The magnetic trapping of cold ground-state antihydrogen (see Figure 1) paved the way for precision spectroscopy experiments using similar laser techniques as for the regular hydrogen [47]. The narrow-line radiation of frequency-stabilized laser at 243 nm was used for two-photon excitation of the 1S–2S transition in trapped antihydrogen. The atoms in the 1S ground state ($F = 1\, m_F = +1$, one of the two trappable states) were exposed by a 300 s laser pulse at the fixed frequency. Frequency-dependent excitation efficiency of the 2S state was extracted from the number of excited and surviving atoms in the ground state after the laser pulse. The spectral line was fitted by the elaborated line shape which allowed extracting the line center frequency corresponding to the trap magnetic field. There were two successful measurement runs at CERN, and the results were published in 2017 [48] and 2018 [49] with the uncertainty reduced by two orders of magnitude compared to the first one. Precision 243 nm two-photon spectroscopy allowed to measure the frequency of the $1S(F = 1, m_F = +1) \rightarrow 2S(F = 1, m_F = +1)$ transition of

$$f_{1S-2S}(\bar{H}) = 2466061103079.4(5.4)\,\text{kHz} \tag{6}$$

in the magnetic field of 1.03285(53) T (the minimum field in the magnetic bottle). The dominating uncertainty contributions are the modeling (the lineshape, the magnetic field distribution, the Stark shift, etc.) and the statistics.

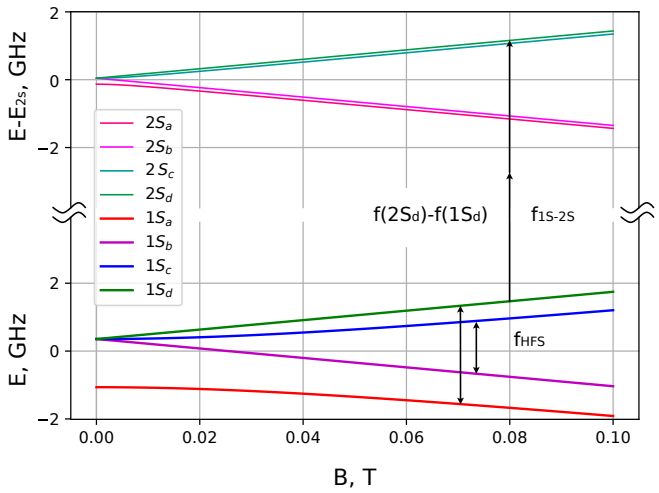

Figure 1. 1S and 2S levels energy in H ($\bar{H}$) in external magnetic field. Atoms in states with indexes "c" and "d" can be confined in a magnetic trap. Commonly used transitions for optical two-photon 1S–2S and microwave hyperfine structure spectroscopy are shown.

Correcting the unperturbed 1S–2S transition frequency in regular hydrogen [47] by the hyperfine and the Zeeman shifts one obtains the frequency of

$$f_{1S-2S}(H) = 2466061103080.3(0.6)\,\text{kHz} \tag{7}$$

corresponding to the same experimental conditions as for antihydrogen (the magnetic field distribution). The uncertainty of (7) results from the magnetic field characterization. Let us remind the reader that the 1S–2S frequency was accurately measured with the relative uncertainty of 4×10^{-15} (or 11 Hz in absolute units) [47,50] by two-photon spectroscopy on the cold atomic beam of H. Compared to the antihydrogen, it is approximately 500 times more accurate, which will stimulate research for further improvement of antihydrogen spectroscopy.

The two frequencies (6) and (7) are consistent within the combined experimental uncertainty of 2×10^{-12} which indicates the high identity of hydrogen and antihydrogen. According to [18], comparison of these frequencies allows for setting the restriction to the Rydberg's ratio of antihydrogen and hydrogen similar to (2)

$$\bar{Ry}(\bar{H}) = \frac{m_{\bar{e}}}{m_e}\frac{m_{\bar{p}}}{m_p}\frac{m_e + m_p}{m_{\bar{e}} + m_{\bar{p}}}\left(\frac{q_{\bar{p}}}{q_p}\right)^2\left(\frac{q_{\bar{e}}}{q_e}\right)^2 \approx \frac{m_{\bar{e}}}{m_e}\left(\frac{q_{\bar{p}}}{q_p}\right)^2\left(\frac{q_{\bar{e}}}{q_e}\right)^2, \tag{8}$$

taking into account that $m_p(m_{\bar{p}})/m_e(m_{\bar{e}}) \approx 1837$, while the known uncertainties of corresponding mass ratios are nearly equivalent (on the order of 10^{-9}). All the ratios contributing to the right side are measured in the other independent measurements with the uncertainties also on the order of 10^{-9}. The question is which of the restrictions can be further improved using antihydrogen spectroscopy, taking into account that $\bar{Ry}(\bar{H})$ differs from the unit by only 2×10^{-12}.

One can combine results of optical spectroscopy in positronium and anti-hydrogen (2) and (8) excluding the positron-to-electron charge ratio:

$$\frac{\bar{Ry}(\bar{H})}{\bar{Ry}(Ps)} = \left(\frac{m_{\bar{e}}}{m_e} + 1\right)\left(\frac{q_{\bar{p}}}{q_p}\right)^2. \tag{9}$$

The restriction to the anti-proton-to-proton charge ratio $q_{\bar{p}}/q_p$ can be derived from the combination of the results from Table 1 (the first part) and Equation (4). Combining independent experiments on regular matter [19] and anti-hydrogen neutrality [34] together with measurement of the positron g-factor [29] one gets $|-q_{\bar{p}}/q_p - 1| < 1.1 \times 10^{-9}$. Using the regular error penetration, one can get from (9) the restriction for the electron-to-positron mass ratio of 7.4×10^{-9} which is basically the same as from (5). It is clear, that without improvement of the charge ratios, further progress in antihydrogen 1S–2S spectroscopy cannot bring a significant contribution to the electron-to-positron mass ratio. On the other hand, the antihydrogen 1S–2S spectroscopy, being the completely independent measurement, brings additional confidence to this result. The numbers given in our analysis are very close to the recently published compilation [51], where the limitation is 8×10^{-9}.

One can refuse the model-independent approach and assume that there are no violations in the electromagnetic sector. The nuclear effects contribute to the 1S–2S frequency in anti-hydrogen via charge distribution of the proton. The energy of hydrogen atomic level can be written as:

$$E_{nlj} = Ry\Big(-\frac{1}{n^2} + f_{nlj}(\alpha, \frac{m_e}{m_p}, \dots) + \frac{C_{NS}}{n^3}\delta_{l0}\langle r_p^2\rangle\Big), \tag{10}$$

where n, l, j are the quantum numbers, $\langle r_p\rangle$ is the charge radius and C_{NS} is a constant [52]. Assuming that matter/anti-matter violation can be buried exclusively in $\langle r_p\rangle$, one can deduce the limitation from antihydrogen spectroscopy.

According to [52], the size of the charge radius contribution to the 1S–2S frequency equals $1.3684\langle r_p\rangle^2$ MHz, where $\langle r_p\rangle$ is measured in fm. The proton charge radius itself equals $\langle r_p\rangle = 0.84184(36)(56)$ fm as measured in [53]. Corresponding contribution to the 1S–2S frequency equals 0.96 MHz or 4×10^{-10} of the 1S–2S frequency (8). One can set a limit to the antiproton-to-proton charge radius ratio of $|\langle r_{\bar{p}}\rangle/\langle r_p\rangle/-1| < 2.5 \times 10^{-3}$. Note, that the proton charge "puzzle" is on the level of 1% [53] which indicates that antiproton and proton are very identical at that level of uncertainty for the absolute value.

The anticipated improvements of anti-hydrogen 1S–2S spectroscopy are expected in the coming years, which will be achieved by better statistics (ELENA anti-matter factory at CERN) and laser cooling of anti-hydrogen [54]. Even achieving the accuracy of regular hydrogen of 10^{-15} these experiments, being really on the very edge of modern physics, will only moderately contribute to the matter-anti-matter symmetry problem.

3.3. Antihydrogen, Hyperfine and the Lamb Shift

As discussed above, the Coulomb interaction contributes to many orders of magnitude to the 1S–2S energy splitting and all other effects remain small at that level. By choosing other atomic levels one can increase their weight where violations may be more probable. One of the prominent candidates is the ground-state hyperfine (HFS) transition (see Figure 1) at 1.42 GHz. The present accuracy of ground state HFS in regular H is at 1 mHz, or 7×10^{-13} in relative frequency units [55]. At the same time, the best measurement in antihydrogen [56] achieved the uncertainty of 0.5 MHz (4×10^{-4}), which was limited by the stability of the magnetic field of the trap. HFS comes from the magnetic interaction of e ($\bar{e}$) with p ($\bar{p}$), which are equivalent to 3.6×10^{-9} level (see g-factor ratios in Table 1). Meantime, the finite size effects (the finite electric and the magnetic radii, the recoil corrections, and the polarizability of p ($\bar{p}$)) contribute at ~33 ppm level [57]. Hence, $\bar{p}$ hyperfine spectroscopy at ppm level should provide a comparison of Zemach radii of p ($\bar{p}$) at a few percent level.

The Lamb shift measurement in antihydrogen in combination with the 1S–2S transition can provide independent information about the antiproton charge radius (similar to hydrogen [58]). It is worth noting that to determine antiproton charge radius with 10% accuracy one needs the Lamb shift measurements at ~30 ppm level, which is far from a near-future capability.

4. Gravitational Tests

Gravitation interaction can also cause matter/anti-matter symmetry breaking. Being the weakest among all four fundamental interactions, it is the one that is the most difficult to test in the laboratory since no bulk anti-matter is available. Similarly, there are no known anti-matter objects in space, which limits the possibility to get information from astrophysical observations.

It is known that the dominating contribution to the mass of baryonic matter (e.g., proton) arises from quark and gluon dynamics, while the quark masses themselves contribute to only 1% of the mass [59]. One can argue that based on this model, matter and anti-matter masses must have similar nature to 99% and Eotvos experiments aimed at testing the Einstein equivalent principle do significantly contribute to the matter/anti-matter gravity problem [60–62]. According to their analysis, the authors infer that any observable gravivector acceleration of antimatter is less than 2×10^{-6} g , where g is a free fall acceleration.

Another interesting observation follows from the 1S–2S spectroscopy in hydrogen/anti-hydrogen concerning the gravitational redshift. The frequency shift Δf in the gravitational potential difference ΔU is given by $\Delta f/f = \Delta U/c^2$. Relative to the zero potential in the infinity, the Earth's gravitational potential on the surface equals $\Delta U_E/c^2 = 6.5 \times 10^{-10}$. The sun's potential is 15 times larger $\Delta U_S/c^2 = 1 \times 10^{-8}$. Knowing, that the 1S–2S frequencies in hydrogen and anti-hydrogen are equivalent to 2×10^{-12}, this spectroscopy experiment tests the gravitational redshift for matter and anti-matter to the level of 2×10^{-4}. Note, that the most accurate test of the gravitational redshift prediction from general relativity is at 2.5×10^{-5} level [63].

Direct measurements of matter/anti-matter gravitational interaction are extremely difficult. Charged particles can not be used because of the strong influence of electromagnetic forces. "Weighting" of the neutral anti-hydrogen seems to be the most straightforward way, but technical difficulties are huge because even at 4 K, the thermal velocity of antihydrogen is around 300 m/s.

In 2013, the ALPHA collaboration managed to deduce the upper limit for antihydrogen mass by analyzing particle dynamics after releasing them from the trap [64]. The derived upper limit for the antihydrogen gravitational mass is 75 of the inertial mass. Being a very important step forward to "weighting" of anti-hydrogen, this restriction can not contribute to the problem of symmetry breaking.

There are several experiments aimed at precise measurement of anti-hydrogen gravitation which requires very cold atoms. GBAR collaboration works on sympathetic cooling of positively charged antihydrogen ($\bar{p} + 2\bar{e}$) down to 10 μK which must drastically increase the sensitivity to gravitation acceleration measurements [65]. The ongoing ALPHA-g experiment at CERN targets a similar purpose [66]. Hopefully, these challenging experiments give a new and more definite understanding of gravitational interaction with anti-matter.

5. Conclusions

In this paper, we restricted our discussion to anti-hydrogen and its comparison to other simple atomic systems like hydrogen and positronium. Impressive spectroscopic results achieved in anti-hydrogen demonstrate great progress in anti-hydrogen synthesis, cooling, and trapping. Still, a comparison with optical transitions in hydrogen provides knowledge mainly about electromagnetic interactions which is only one of the feasible sources of parity violations. Using a model-independent approach, one can basically deduce the restriction for the electron-to-positron mass ratio of 7.4×10^{-9}. The expected improvement of the 1S–2S frequency in antihydrogen will not directly bring an improvement for this fundamental ratio without further progress in positronium spectroscopy and improvements of charge ratios. Searching for informative violations in the electromagnetic sector seems very challenging, knowing that there is no observed CPT violation at $\Delta m/m < 10^{-18}$ level obtained from measurements of decay channels of the neutral $K^0/\bar{K}^0$ mesons [67]. Direct

measurements of the gravitational behavior of antimatter are very intriguing, although it is hard to expect big surprises like "anti-gravity".

It seems that searching for and studying matter/anti-matter violations will remain a challenge for many years, covering a wide range of different theoretical approaches, and astrophysical and laboratory experiments. Today's laboratory techniques developed for manipulation with anti-matter allow for a significant improvement of current limitations, but it is hard to predict at which level one may expect the violation and how many orders of magnitude need to fill the gap.

Author Contributions: K.K.: Data analysis (antihydrogen 1S–2S part), manuscript writing; A.G.: Data verification (antihydrogen heyperfine spectrosopy part), manuscript writing, figures presentation; N.K.: Data analysis (positronium and elementary particles), manuscript writing (introduction, tables), general concept of the manuscript. All authors have read and agreed to the published version of the manuscript.

Funding: This research received no external funding.

Data Availability Statement: No new data were created or analyzed in this study. Data sharing is not applicable to this article.

Conflicts of Interest: The authors declare no conflict of interest.

References

1. Dirac, P.A.M. The quantum theory of the electron. *Proc. R. Soc. Lond. A* **1928**, *117*, 610.
2. Anderson, C.D. The apparent existence of easily deflectable positives. *Science* **1932**, *76*, 238–239. [CrossRef]
3. Shong, J.A.D., Jr.; Hildebrand, R.H.; Meyer, P. Ratio of electrons to positrons in the primary cosmic radiation. *Phys. Rev. Lett.* **1964**, *12*, 3. [CrossRef]
4. Adriani, O.; Barbarino, G.C.; Bazilevskaya, G.A.; Bellotti, R.; Boezio, M.; Bogomolov, E.A.; Bonechi, L.; Bongi, M.; Bonvicini, V.; Borisov, S.; et al. PAMELA measurements of cosmic-ray proton and helium spectra. *Science* **2011**, *332*, 69–72. [CrossRef] [PubMed]
5. Ackermann, M.; Ajello, M.; Allafort, A.; Atwood, W.B.; Baldini, L.; Barbiellini, G.; Bastieri, D.; Bechtol, K.; Bellazzini, R.; Berenji, B.; et al. Measurement of Separate Cosmic-Ray Electron and Positron Spectra with the Fermi Large Area Telescope. *Phys. Rev. Lett.* **2012**, *108*, 011103. [CrossRef] [PubMed]
6. Aguilar, M.; Cavasonza, L.A.; Alpat, B.; Ambrosi, G.; Arruda, L.; Attig, N.; Aupetit, S.; Azzarello, P.; Bachlechner, A.; Barao, F.; et al. First Result from the Alpha Magnetic Spectrometer on the International Space Station: Precision Measurement of the Positron Fraction in Primary Cosmic Rays of 0.5–350 GeV. *Phys. Rev. Lett.* **2013**, *110*, 141102. [CrossRef] [PubMed]
7. Haymes, R.C.; Ellis, D.V.; Fishman, G.J.; Glenn, S.W.; Kurfess, J.D. Observation of hard radiation from the region of the Galactic Center. *Astrophys. J.* **1969**, *157*, 1455. [CrossRef]
8. Knödlseder, J.; Jean, P.; Lonjou, V.; Weidenspointner, G.; Guessoum, N.; Gillard, W.; Skinner, G.; von Ballmoos, P.; Vedrenne, G.; Roques, J.-P.; et al. The all-sky distribution of 511 keV electron-positron annihilation emission. *Astron. Astrophys.* **2005**, *441*, 513–532. [CrossRef]
9. Golden, R.L.; Horan, S.; Mauger, B.G.; Badhwar, G.D.; Lacy, J.L.; Stephens, S.A.; Daniel, R.R.; Zipse, J.E. Evidence for the existence of cosmic-ray antiprotons. *Phys. Rev. Lett.* **1979**, *43*, 1196. [CrossRef]
10. Aguilar, M.; Cavasonza, L.A.; Alpat, B.; Ambrosi, G.; Arruda, L.; Attig, N.; Aupetit, S.; Azzarello, P.; Bachlechner, A.; Barao, F.; et al. Antiproton flux, antiproton-to-proton flux ratio, and properties of elementary particle fluxes in primary cosmic rays measured with the alpha magnetic spectrometer on the international space station. *Phys. Rev. Lett.* **2016**, *117*, 091103. [CrossRef]
11. Canetti, L.; Drewes, M.; Shaposhnikov, M. Matter and Antimatter in the Universe. *New J. Phys.* **2012**, *14*, 095012. [CrossRef]
12. Fortson, E.N.; Lewis, L.L. Atomic parity nonconservation experiments. *Phys. Rep.* **1984**, *113*, 289–344. [CrossRef]
13. Cairncross, W.B.; Gresh, D.N.; Grau, M.; Cossel, K.C.; Roussy, T.S.; Ni, Y.; Zhou, Y.; Cornell, E.A. Precision measurement of the electron's electric dipole moment using trapped molecular ions. *Phys. Rev. Lett.* **2017**, *119*, 153001. [CrossRef] [PubMed]
14. Fischer, M.; Kolachevsky, N.; Zimmermann, M.; Holzwarth, R.; Udem, T.; Hänsch, T.W.; Abgrall, M.; Grünert, J.; Maksimovic, I.; Bize, S. et al. New limits on the drift of fundamental constants from laboratory measurements. *Phys. Rev. Lett.* **2004**, *92*, 230802. [CrossRef]
15. Hohensee, M.A.; Leefer, N.; Budker, D.; Harabati, C.; Dzuba, V.A.; Flambaum, V.V. Limits on violations of Lorentz symmetry and the Einstein equivalence principle using radio-frequency spectroscopy of atomic dysprosium. *Phys. Rev. Lett.* **2013**, *111*, 050401. [CrossRef] [PubMed]
16. Derevianko, A.; Pospelov, M. Hunting for topological dark matter with atomic clocks. *Nat. Phys.* **2014**, *10*, 933–936. [CrossRef]
17. Safronova, M.S.; Budker, D.; DeMille, D.; Kimball, D.F.J.; Derevianko, A.; Clark, C.W. Search for new physics with atoms and molecules. *Rev. Mod. Phys.* **2018**, *90*, 025008. [CrossRef]
18. Hughes, R.J.; Deutch, B.I. Electric charges of positrons and antiprotons. *Phys. Rev. Lett.* **1992**, *69*, 578. [CrossRef] [PubMed]

19. Bressi, G.; Carugno, G.; Della Valle, F.; Galeazzi, G.; Ruoso, G.; Sartori, G. Testing the neutrality of matter by acoustic means in a spherical resonator. *Phys. Rev. A* **2011**, *83*, 052101. [CrossRef]
20. Borchert, M.J.; Devlin, J.A.; Erlewein, S.R.; Fleck, M.; Harrington, J.A.; Higuchi, T.; Latacz, B.M.; Voelksen, F.; Wursten, E.J.; Abbass, F.; et al. A 16-parts-per-trillion measurement of the antiproton-to-proton charge–mass ratio. *Nature* **2022**, *601*, 53–57. [CrossRef]
21. Gabrielse, G.; Khabbaz, A.; Hall, D.S.; Heimann, C.; Kalinowsky, H.; Jhe, W. Precision mass spectroscopy of the antiproton and proton using simultaneously trapped particles. *Phys. Rev. Lett.* **1999**, *82*, 3198. [CrossRef]
22. Hori, M.; Sótér, A.; Barna, D.; Dax, A.; Hayano, R.; Friedreich, S.; Juhász, B.; Pask, T.; Widmann, E.; Horváth, D.; et al. Two-photon laser spectroscopy of antiprotonic helium and the antiproton-to-electron mass ratio. *Nature* **2011**, *475*, 484–488. [CrossRef] [PubMed]
23. Constants. Available online: https://physics.nist.gov/cuu/Constants/ (accessed on 21 July 2023)
24. Bluhm, R.; Kostelecky, V.A.; Russell, N. Theory of the anomalous magnetic moment of the electron. *AIP Conf. Proc.* **1999**, *457*, 138–142.
25. Schwinberg, P.B.; Dyck, R.S.V., Jr.; Dehmelt, H.G. Trapping and thermalization of positrons for geonium spectroscopy. *Phys. Lett. A* **1981**, *81*, 119–120. [CrossRef]
26. Anderson, V.; Rodgers, M.A.; Tsao, D. Measuring Positron Mass Using Gamma-ray Detection of Electron-positron Annihilation (Unpublished). Available online: https://studylib.net/doc/5878297/measuring-positron-mass-using-gamma (accessed on 21 July 2023).
27. Aoyama, T.; Kinoshita, T.; Nio, M. Theory of the anomalous magnetic moment of the electron. *Atoms* **2019**, *7*, 28. [CrossRef]
28. Fan, X.; Myers, T.G.; Sukra, B.A.D.; Gabrielse, G. Measurement of the electron magnetic moment. *Phys. Rev. Lett.* **2023**, *130*, 071801. [CrossRef]
29. Dyck, R.S.V., Jr.; Schwinberg, P.B.; Dehmelt, H.G. New high-precision comparison of electron and positron g factors. *Phys. Rev. Lett.* **1987**, *59*, 26. [CrossRef]
30. DiSciacca, J.; Gabrielse, G. Direct measurement of the proton magnetic moment. *Phys. Rev. Lett.* **2012**, *108*, 153001. [CrossRef]
31. Mooser, A.; Ulmer, S.; Blaum, K.; Franke, K.; Kracke, H.; Leiteritz, C.; Quint, W.; Rodegheri, C.C.; Smorra, C.; Walz, J. Direct high-precision measurement of the magnetic moment of the proton. *Nature* **2014**, *509*, 596–599. [CrossRef]
32. Schneider, G.; Mooser, A.; Bohman, M.; Schön, N.; Harrington, J.; Higuchi, T.; Nagahama, H.; Sellner, S.; Smorra, C.; Blaum, K.; et al. Double-trap measurement of the proton magnetic moment at 0.3 parts per billion precision. *Science* **2017**, *358*, 1081–1084. [CrossRef]
33. Smorra, C.; Sellner, S.; Borchert, M.J.; Harrington, J.A.; Higuchi, T.; Nagahama, H.; Tanaka, T.; Mooser, A.; Schneider, G.; Bohman, M.; et al. A parts-per-billion measurement of the antiproton magnetic moment. *Nature* **2017**, *550*, 371. [CrossRef] [PubMed]
34. Ahmadi, M.; Baquero-Ruiz, M.; Bertsche, W.; Butler, E.; Capra, A.; Carruth, C.; Cesar, C.L.; Charlton, M.; Charman, A.E.; Eriksson, S.' et al. An improved limit on the charge of antihydrogen from stochastic acceleration. *Nature* **2016**, *529*, 373–376. [CrossRef] [PubMed]
35. Roberts, B.M.; Blewitt, G.; Dailey, C.; Murphy, M.; Pospelov, M.; Rollings, A.; Sherman, J.; Williams, W.; Derevianko, A. Search for domain wall dark matter with atomic clocks on board global positioning system satellites. *Nat. Commun.* **2017**, *8*, 1195. [CrossRef] [PubMed]
36. Kobayashi, T.; Takamizawa, A.; Akamatsu, D.; Kawasaki, A.; Nishiyama, A.; Hosaka, K.; Hisai, Y.; Wada, M.; Inaba, H.; Tanabe, T.; et al. Search for ultralight dark matter from long-term frequency comparisons of optical and microwave atomic clocks. *Phys. Rev. Lett.* **2022**, *129*, 241301. [CrossRef]
37. Chu, S.; Mills, A.P., Jr.; Hall, J.L. Measurement of the Positronium $1^3S_1 \rightarrow 2^3S_1$ Interval by Doppler-Free Two-Photon Spectroscopy. *Phys. Rev. Lett.* **1984**, *52*, 1689. [CrossRef]
38. Fee, M.S.; Chu, S.; Mills, A.P., Jr.; Chichester, R.J.; Zuckerman, D.M.; Shaw, E.D.; Danzmann, K. Measurement of the positronium $1^3S_1 \rightarrow 2^3S_1$ interval by continuous-wave two-photon excitation. *Phys. Rev. A* **1993**, *48*, 192. [CrossRef]
39. Adkins, G.S.; Kim, M.; Parsons, C.; Fell, R.N. Three-photon-annihilation contributions to positronium energies at order $m\alpha^7$. *Phys. Rev. Lett.* **2015**, *115*, 233401. [CrossRef]
40. Amsler, C.; Antonello, M.; Belov, A.; Bonomi, G.; Brusa, R.S.; Caccia, M.; Camper, A.; Caravita, R.; Castelli, F.; Cerchiari, G.; et al. Velocity-selected production of 2^3S metastable positronium. *Phys. Rev. A* **2019**, *99*, 033405. [CrossRef]
41. Babij, T.J., Cassidy, D.B. Positronium microwave spectroscopy using Ramsey interferometry. *Eur. Phys. J. D* **2022**, *76*, 121. [CrossRef]
42. Crivelli, P.; Wichmann, G. Positronium and Muonium 1S–2S laser spectroscopy as a probe for the standard-model extension. *arXiv* **2016**, arXiv:1607.06398.
43. Baur, G.A.; Boero, G.; Brauksiepe, A.; Buzzo, A.; Eyrich, W.; Geyer, R.; Grzonka, D.; Hauffe, J.; Kilian, K.; LoVetere, M.; et al. Production of antihydrogen. *Phys. Lett. B* **1996**, *368*, 251–258. [CrossRef]
44. Andresen, G.B.; Ashkezari, M.D.; Baquero-Ruiz, M.; Bertsche, W.; Bowe, P.D.; Butler, E.; Cesar, C.L.; Chapman, S.; Charlton, M.; Deller, A.; et al. Trapped antihydrogen. *Nature* **2010**, *468*, 673. [CrossRef] [PubMed]
45. Andresen, G.B.; Ashkezari, M.D.; Baquero-Ruiz, M.; Bertsche, W.; Bowe, P.D.; Butler, E.; Cesar, C.L.; Chapman, S.; Charlton, M.; Deller, A.; et al. Confinement of antihydrogen for 1000 s. *Nat. Phys.* **2011**, *7*, 558–564.

46. Gabrielse, G.; Kalra, R.; Kolthammer, W.S.; McConnell, R.; Richerme, P.; Grzonka, D.; Oelert, W.; Sefzick, T.; Zielinski, M.; Fitzakerley, D.W.; et al. Trapped antihydrogen in its ground state. *Phys. Rev. Lett.* **2012**, *108*, 113002. [CrossRef] [PubMed]
47. Parthey, C.G.; Matveev, A.; Alnis, J.; Bernhardt, B.; Beyer, A.; Holzwarth, R.; Maistrou, A.; Pohl, R.; Predehl, K.; Udem, T.; et al. Improved measurement of the hydrogen 1S–2S transition frequency. *Phys. Rev. Lett.* **2011**, *107*, 203001. [CrossRef]
48. Ahmadi, M.; Alves, B.X.R.; Baker, C.J.; Bertsche, W.; Butler, E.; Capra, A.; Carruth, C.; Cesar, C.L.; Charlton, M.; Cohen, S.; et al. Observation of the 1S–2S transition in trapped antihydrogen. *Nature* **2017**, *541*, 506–510. [CrossRef]
49. Ahmadi, M.; Alves, B.X.R.; Baker, C.J.; Bertsche, W.; Capra, A.; Carruth, C.; Cesar, C.L.; Charlton, M.; Cohen, S.; et al. Characterization of the 1S–2S transition in antihydrogen. *Nature* **2018**, *557*, 71–75. [CrossRef]
50. Matveev, A.; Parthey, C.G.; Predehl, K.; Alnis, J.; Beyer, A.; Holzwarth, R.; Udem, T.; Wilken, T.; Kolachevsky, N.; Abgrall, M.; et al. Precision measurement of the hydrogen 1S–2S frequency via a 920-km fiber link. *Phys. Rev. Lett.* **2013**, *110*, 230801. [CrossRef]
51. Zyla, P.A.; Barnett, R.M.; Beringer, J.; Particle Data Group. Review of Particle Physics. *Prog. Theor. Exp. Phys.* **2020**, *2020*, 083C01.
52. Khabarova, K.; Kolachevsky, N. Proton charge radius. *Phys. Uspekhi* **2021**, *64*, 1038. [CrossRef]
53. Pohl, R.; Antognini, A.; Nez, F.; Amaro, F.D.; Biraben, F.; Cardoso, J.M.; Covita, D.S.; Dax, A.; Dhawan, S.; Fernandes, L.M.P.; et al. The size of the proton. *Nature* **2010**, *466*, 213–216. [CrossRef] [PubMed]
54. Baker, C.J.; Bertsche, W.; Capra, A.; Carruth, C.; Cesar, C.L.; Charlton, M.; Christensen, A.; Collister, R.; Mathad, A.C.; Eriksson, S.; et al. Laser cooling of antihydrogen atoms. *Nature* **2021**, *592*, 35–42. [CrossRef] [PubMed]
55. Petit, P.; Desaintfuscien, M.; Audoin, C. Temperature dependence of the hydrogen maser wall shift in the temperature range 295–395 K. *Metrologia* **1980**, *16*, 7. [CrossRef]
56. Ahmadi, M.; Alves, B.X.R.; Baker, C.J.; Bertsche, W.; Butler, E.; Capra, A.; Carruth, C.; Cesar, C.L.; Charlton, M.; Cohen, S.; et al. Observation of the hyperfine spectrum of antihydrogen. *Nature* **2017**, *548*, 66–69. [CrossRef] [PubMed]
57. Carlson, C.E.; Nazaryan, V.; Griffioen, K. Proton structure corrections to electronic and muonic hydrogen hyperfine splitting. *Phys. Rev. A* **2008**, *78*, 022517. [CrossRef]
58. Bezginov, N.; Valdez, T.; Horbatsch, M.; Marsman, A.; Vutha, A.C.; Hessels, E.A. A measurement of the atomic hydrogen Lamb shift and the proton charge radius. *Science* **2019**, *365*, 1007–1012. [CrossRef]
59. Yang, Y.B.; Liang, J.; Bi, Y.J.; Chen, Y.; Draper, T.; Liu, K.F.; Liu, Z. Proton mass decomposition from the QCD energy momentum tensor. *Phys. Rev. Lett.* **2018**, *121*, 212001. [CrossRef]
60. Nieto, M., Goldman, T. The arguments against "antigravity" and the gravitational acceleration of antimatter *Phys. Rep.* **1991**, *205*, 221–281. [CrossRef]
61. Adelberger, E.G.; Heckel, B.R.; Stubbs, C.W.; Su, Y. Does antimatter fall with the same acceleration as ordinary matter? *Phys. Rev. Lett.* **1991**, *66*, 850. [CrossRef]
62. Huber, F.M.; Lewis, R.A.; Messerschmid, E.W.; Smith, G.A. Precision tests of Einstein's Weak Equivalence Principle for antimatter. *Adv. Space Res.* **2000**, *25*, 1245–1249. [CrossRef]
63. Delva, P.; Puchades, N.; Schönemann, E.; Dilssner, F.; Courde, C.; Bertone, S.; Gonzalez, F.; Hees, A.; Le Poncin-Lafitte, C.; Meynadier, F.; et al. Gravitational redshift test using eccentric Galileo satellites. *Phys. Rev. Lett.* **2018**, *121*, 231101. [CrossRef] [PubMed]
64. The ALPHA Collaboration; Charman, A.E. Description and first application of a new technique to measure the gravitational mass of antihydrogen. *Nat. Commun.* **2013**, *4*, 1785. [PubMed]
65. Perez, P.; Banerjee, D.; Biraben, F.; Brook-Roberge, D.; Charlton, M.; Cladé, P.; Comini, P.; Crivelli, P.; Dalkarov, O.; Debu, P.; et al. The GBAR antimatter gravity experiment. *Hyperfine Interact.* **2015**, *233*, 21–27. [CrossRef]
66. So, C.; Fajans, J.; Bertsche, W. The ALPHA-g antihydrogen gravity magnet system. *IEEE Trans. Appl. Supercond.* **2020**, *30*, 1–5. [CrossRef]
67. Schwingenheuer, B.; Briere, R.A.; Barker, A.R.; Cheu, E.; Gibbons, L.K.; Harris, D.A.; Makoff, G.; McFarl, K.S.; Roodman, A.; Wah, Y.W.; et al. CPT tests in the neutral kaon system. *Phys. Rev. Lett.* **1995**, *74*, 4376. [CrossRef]